

## NUMERICAL ANALYSIS OF HELICOPTER'S BLADE PITCH LINK LOADS

Alexandre MADEIRA, [Alexandre.madeira@airbus.com](mailto:Alexandre.madeira@airbus.com),<sup>1,2</sup>  
 Lionel ROUCOULES, [Lionel.roucoules@ensam.eu](mailto:Lionel.roucoules@ensam.eu),<sup>1</sup>  
 François MALBURET, [francois.malburet@ensam.eu](mailto:francois.malburet@ensam.eu),<sup>1</sup>  
 Christophe SERR, [christophe.serr@airbus.com](mailto:christophe.serr@airbus.com),<sup>2</sup>  
 Manousos KELAIDIS, [manousos.kelaidis@airbus.com](mailto:manousos.kelaidis@airbus.com),<sup>2</sup>

<sup>1</sup> Arts et Métiers Institute of Technology, LISPEN EA 7515, HeSam, Aix-en-Provence, France

<sup>2</sup> Airbus Helicopters, Loads and Flight Mechanic department, 13725 Marignane Cedex, France

### Abstract

The industrial process for the design of main rotor blades is more and more challenging. Taking into account the loads aspect in the blade design process became necessary to ensure a blade design that can be relevant with a high-speed usage. This paper presents the last results of recent studies about pitch link loads. Within the framework of the CHALLENGE AeRothermoMEchanique project (CHARME) an important study has been made in order to understand and to improve the control loads prediction capability. The first part of this work was to identify the correct model to be used. A large study was done in order to understand different model's effects, validity domain and relevance. The main goal of this part was to identify the most relevant aerodynamic modeling base to be used for the next step. All the models used are included in our global aeromechanic code. The second part of the work was to use this modeling base to identify the blade's pitch link load of a state-of-the-art main rotor blade during a high-speed forward flight.

### 1. NOTATIONS

$C_d, C_l, C_m$	Airfoil aerodynamic coefficients
$C_{zm}$	Mean rotor lift coefficient
$\psi$	Blade's azimuthal position (deg.)
$Re$	Reynolds number
$A$	Sideslip angle (deg.)
$K_A$	Sideslip correction parameter
$AoA$	Angle of attack (deg.)
$\alpha, \dot{\alpha}, \ddot{\alpha}$	AoA & time derivatives
$HOST$	Helicopter Overall Simulation Tool
$FISUW$	Finite state unsteady wake model
$daN$	Decanewton

### 2. INTRODUCTION

Pitch link load calculation is more and more challenging. Recent aircraft developments have shown the importance of an accurate pitch link load's prediction. However many models and correction models compose the HOST [1] aeromechanic code. It becomes difficult to clearly know which model to use and why. This assessment led us to the CHARME research program whose goal is to improve load prediction capabilities. This paper will present recent study results and the possible new ways of working concerning blade pitch link load calculation. First, the paper will present the current pitch link load method applied to a high-speed forward flight. Then a modelling base, chosen within the framework of CHARME, will be presented and explained. The chosen models will be applied to a high-speed forward flight, analyzed and compared to the current pitch link loads calculation method. Then, the paper will present the possibilities for future works.

### 3. CURRENT CALCULATION METHOD

In this part, we will use the most frequently used modelling base on the high-speed forward flight. For several years, the mostly used induced velocity model is FISUW [2]. This model allows variable harmonic and polynomial settings for the computation of the inflow. We can easily change the settings depending on the goal of the study (accuracy or time computation).

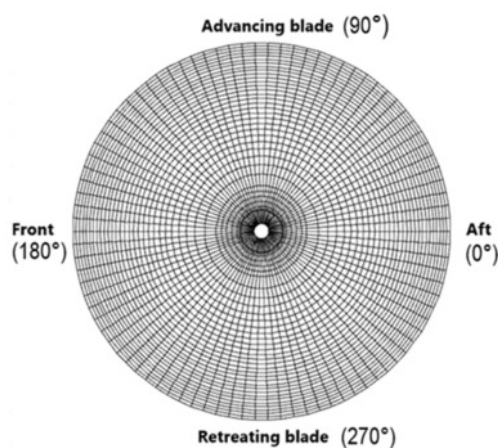


Figure 1: Conventions for main rotor mapping reading

This induced velocity model is associated to other secondary models whose goals are to make relevant two-dimensional airfoil characteristics in a three dimensions environment such as sweep correction, Reynolds Number correction and so on. Concerning the aeromechanic code, HOST allows different types of calculation:

- Trim calculation
- Trim in time marching simulation
- Direct control in time marching simulation
- Indirect control in time marching simulation

For main rotor loads computation, equilibrium is very often selected because of the very low computation time. Besides, the equilibrium's mode allows various parameters sweeping which is extremely useful for load spectrum computation. Furthermore, the blade is assumed as a flexible blade according to the R85 flexible blade model [3].

The chosen flight case is a gyrodyne's 220kt forward flight. We have chosen this flight case because of the conclusion made by P.Eglin and M.Paris about X3's control loads [4]. In fact, an important contribution of the  $C_m$  has been shown in this case, but many questions are still unanswered. Another gyrodyne demonstrator will fly; the RACER and we hope it will allow us to find some answers. Taking into account gyrodyne's specific features, we have decided to use an isolated flat rotor model. The total main rotor thrust is imposed as well as cyclic flapping angle set to zero. Actually, for this type of rotorcraft at such high speed, the main rotor is only used for lifting the aircraft but at a low mean lift coefficient ( $C_{zm}$ ) because wings do an important part of the lifting work.

With those considerations in mind, standard computation is done.

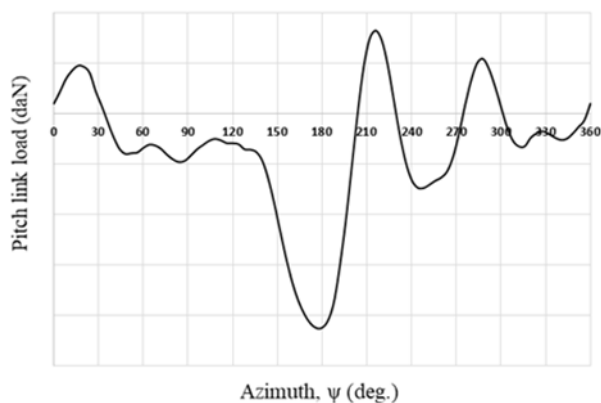


Figure 2: Pitch link load calculated with basic model

In Figure 2 the pitch link load's signal shows important oscillations in retreating blade area (Azimuth,  $\psi$  from  $180^\circ$  to  $360^\circ$ ). Beyond the

interesting analysis that we could do, the major point of this model is that it is difficult to check result's validity.

Actually, some used models are empirical. Our approach will be led by the desire of keeping every models that are based on physical parameters. So, empirical models will be avoided. This way, the results could be more easily compared to flight test results and improvement possibilities could be clearer.

#### 4. NEW MODELLING

The main objective of this part is to identify which model to be used. So it began by an accurate analysis of the mostly used models available in HOST. The work done has shown the result's differences in function of the calculation type (Equilibrium etc.). Results accuracy is better using an equilibrium resolution in time marching simulation. Therefore, this type of resolution will be preferred.

Correction models were compared and selected. Those models are used in HOST in order to introduce some physical parts which are absent in the basic model. Some of them are fully understood [5] but some still require work. In our modelling base, three additional models were chosen because they bring important part of the physics and are without any empirical corrections. So these three models and their impact on the blade pitch link loads are presented.

- Reynolds Number

This model was created in order to take into account the difference between the Reynold's number during airfoil characterization tests and the one in the rotor environment. Airfoil coefficients ( $C_d$ ,  $C_l$  and  $C_m$ ) are interpolated in wind tunnel results database and then corrected by a function depending on the Reynolds number during wind tunnel tests and the one at the considered blade section in operational conditions.

- Sideslip effect

This model was created in order to take into account the 3D behavior of the airfoil from a two-dimensional database. Actually HOST uses wind tunnel airfoil tests results which are static and without 3D effects. However, in the reality some blade sections are subject to AoA and sideslip variations. This model modifies the AoA taken into account for aerodynamic coefficients interpolation.

- Unsteady moment correction

As for sideslip effect, this model was created in order to add the unsteady aerodynamic airfoil behavior. This model is very close to Theodorsen model [6] but has been completed by Kruppa [7], especially for angle of attack time derivative computation. This model only works in the pre stall polar area. Because of the low rotor mean lift coefficient, we assume that the blade's section AoA are low. That is the reason why we do not use dynamic stall model. However, the model exists and could have been chosen for a higher loaded flight case. This model is based on the Tarzanin's theory [8].

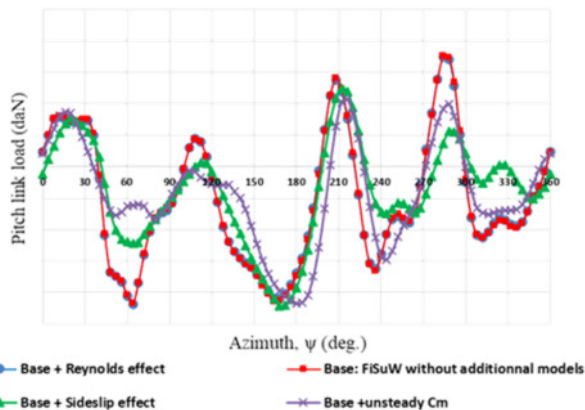


Figure 3: Additional models effect on blade pitch link loads calculation

In Figure 3, additional models effects are visible. Reynolds effect is very low because this correction has just an impact on the drag coefficient ( $C_d$ ). By the way, we identified the model's limit. Because Reynolds number should have an impact on all aerodynamic coefficients. Especially for  $C_l$ , Reynolds effect could change the stall angle of attack and the maximum lift coefficient. The sideslip effect model corrects all airfoil coefficients depending in the sideslip angle value  $\Lambda$ . This model uses a correction process as defined in Figure 4.

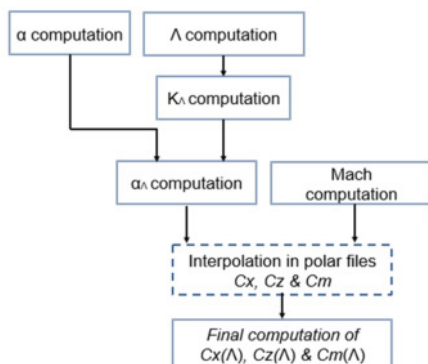


Figure 4: Sideslip correction process

The unsteady  $C_m$  correction depends on the angle of attack temporal derivatives  $\dot{\alpha}$  and  $\ddot{\alpha}$ . It is an important model that adds aerodynamic damping. The effect is clearly visible. The retreating blade oscillations are mainly caused by a torsional response, the  $C_m$  correction allows damping those oscillations.

- Induced velocity models

In addition to those secondary models, induced velocity models can greatly change the results. Several induced velocity models are available in HOST but three of them are the most frequently used:

- Meijer-Drees
- FISUW
- MINT

Meijer-Drees is a well-known simple model [9] and faster to use than others. FISUW (Finite State unsteady wake model) is the result of several years of collaboration between ONERA and AIRBUS. Based on the potential flow theory[2] it is fast to use and accurate. However, it does not take into account the blade wake. MINT[10] was developed from the MESIR model but improved in order to allow time-marched simulations[11]. Its wake model formulation is based on steady thin wake theory. MINT wake model was developed by ONERA taking into account the experience obtained from two other models METAR and MESIR. MINT is based on the Mudry's theory that allows having a detailed description of the unsteady wake evolution modeled by a surface with a discontinuity of speed potential. The wake is discretized in panels. The last version of MINT can be used in two ways, free wake or rigid wake.

Using the modelling base explained in this part, we compare induced velocity models effects on the 220kt forward flight beginning by the comparison between rigid and free wake using in Figure 5.

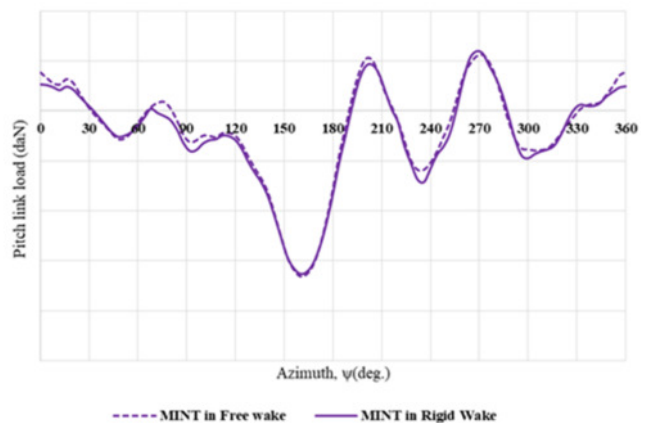


Figure 5: Comparison of results - Free wake and rigid wake

It appears that using free wake model does not seem to be useful. Total blade pitch link signals are extremely close one to the other, but time computation is much higher using free wake model (Rigid wake around 30 minutes, free wake 50 times more). The induced velocity mappings are also very similar.

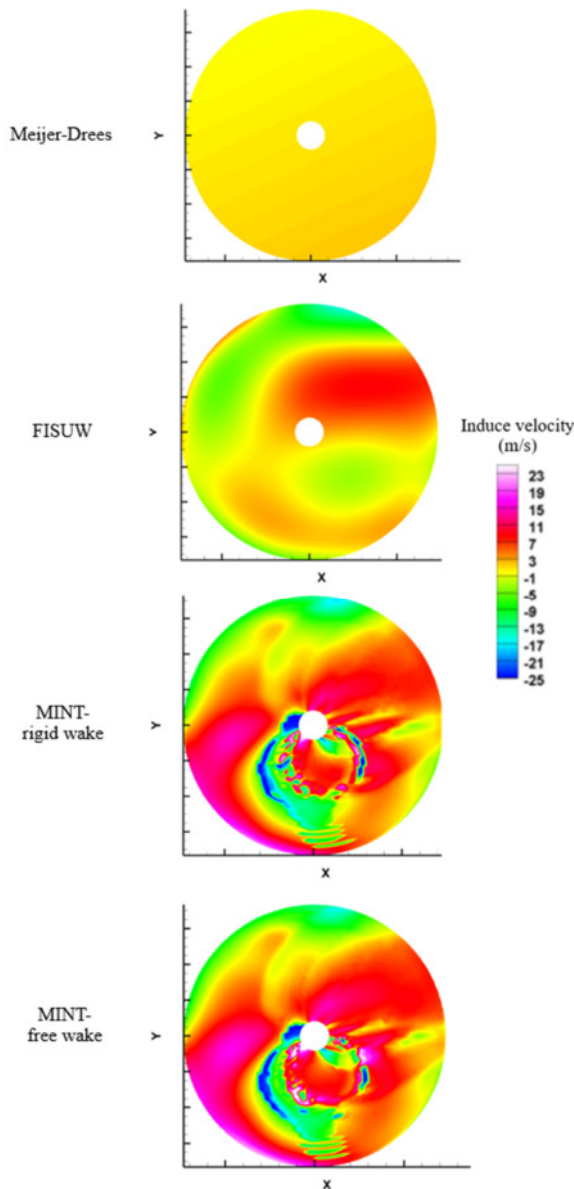


Figure 6: Induced velocity mappings

In Figure 6 effects of the different induced velocity models are shown according to

Figure 1 reading conventions. The Meijer-Drees model gives a linear velocity repartition on the rotor disk. FISUW gives a more complete velocity repartition but still simple mainly because of the low  $C_{zm}$  value and the flat disk assumption which limit the blade cyclic flapping (consistent with the chosen flight case).

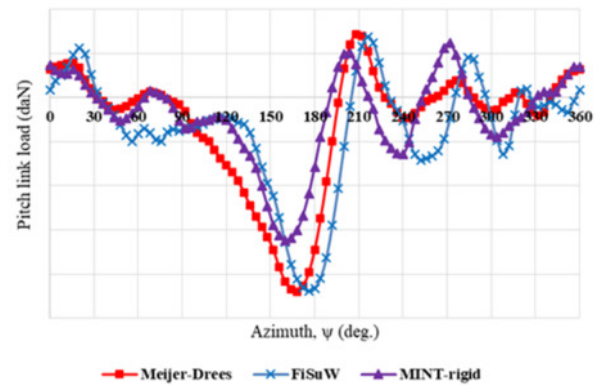


Figure 7: Induced velocity effects on pitch link load

Nevertheless, it is interesting to see that both Meijer-Drees and FISUW give similar pitch link signal's amplitude in the disk's front sector despite different induced velocity values.

As for MINT, results are different. The signal amplitude is lower in the front disk's area and the retreating blade oscillations have different phases.

In this case, MINT adds an important part of the physics that is the wake effect and the blade-vortex interaction. Consequently, we have chosen MINT for further computations.

Nevertheless, we saw some limits especially close to reversed flow disc outline. In these conditions, unphysical peaks of induced velocity can occur. In order to counter this aspect, an induced velocity limitation is used ( $\pm 25$ m/s). In Figure 6, MINT velocity mappings show those induced velocity singularities (in blue dark) drawing the reversed flow disc outline for both free and rigid wake models.

This is an important aspect to deal with. Actually, for a forward flight at high speed (more than 100kt) we assume that a 25 rotor rotations are necessary in order to obtain solution's convergence. Without induced velocity limitation, aerodynamic coefficients would tend to slowly move apart because of local velocity values and AoA. Those coefficients would create important induced velocity values, which would accelerate divergence phenomena. Then, at the end of the 5 seconds computation, induced velocities would be very high (above 100m/s on reverse flow disc outline) and aerodynamic coefficients would be completely unphysical.

This would have an important impact on the control load results. The absolute speed value on the reversed flow disc outline would be well above zero when normally equal to zero with a negligible effect on control loads.

Besides a 25m/s limitation seems to be consistent because it does not limit the induced velocity in relevant main rotor disc areas and it protects from induced velocity singularities. As we saw for both free and rigid wake, the phenomenon is limited to reversed disc outline in this flight case.

## 5. FINAL COMPUTATION AND ANALYSIS

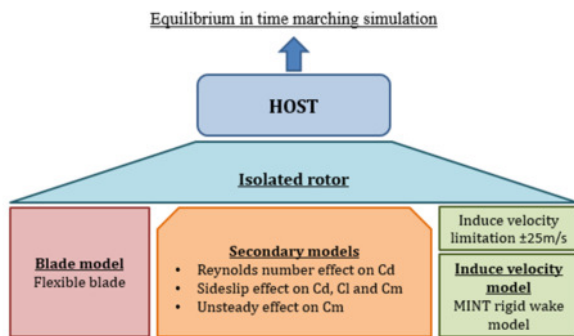


Figure 8 : Chosen modeling base

With the modeling base detailed in Figure 8, we made a new computation using MINT and the three additional models explained before. In this part we will compare the old computation method with the one detailed above.

An important difference between those methods is the resolution type. The previous method only uses the equilibrium resolution, whereas the new method solve the equilibrium but in time marching simulation. This work permitted first to clarify the models we used in order to predict control loads and to improve the model using traceability.

Here we compare the pitch link load's contributions: aerodynamic, inertial and lag damper contributions. In Figure 9, blade pitch link loads and major components are compared for the initial computation and the one done with our new assumptions. The results on the total pitch link load show similar curve shapes but with different amplitude. The aerodynamic part changes a bit and is smoother using the new modeling base. Lead lag damper parts are very similar in both models. It seems that the main amplitude difference comes from the inertial part. The computation made with FISUW shows a more important pitch link compression near  $\psi=180^\circ$  and a phase shift.

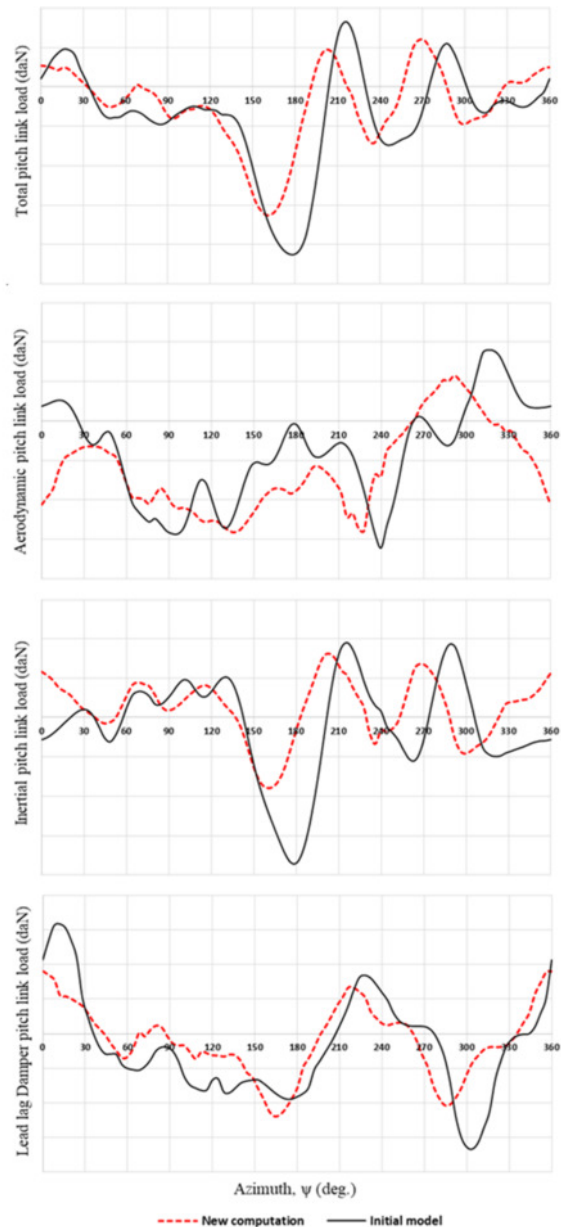


Figure 9 :New computation versus Initial computation & pitch link load's components

This case is very specific because the inertial part here plays an important role, which does not seem to be linked to the aerodynamic part. However, in the new computation results the reversed flow disc effect appears to be more visible while it is invisible with the first modeling method.

- New computation's analysis method

A new analysis tool has been developed within the framework of CHARME research program. This tool allows a new way of post-processing in order to analysis pitch link loads. With this tool, we can now show a new representation of the results given by HOST through a mapping. This way we can easily see where the pitch link load occurs. Figure 10 and Figure 11 show inertial and aerodynamic pitch link load mapping. In the inertial mapping (Figure 10) we can identify the area where the pitch link compression occurs (near  $\psi=160^\circ$ ). In this area, the blade's second mode bending is very important and occurs with a high lead lag dynamic at the same time. This is responsible of the important pitch link compression observed at  $\psi=160^\circ$ . The load concentration is caused by the tuning mass used in order to balance the blade (dynamic tuning).

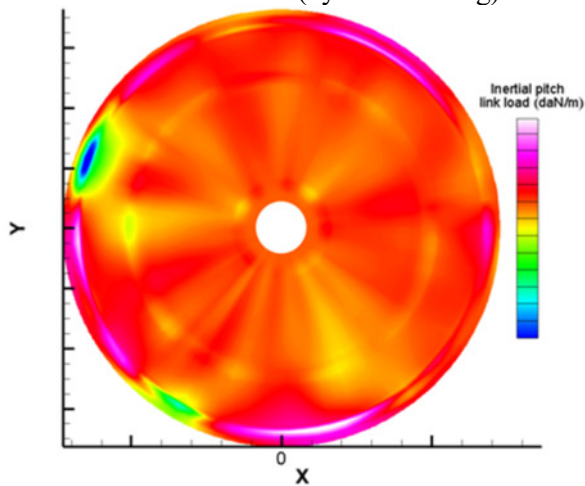


Figure 10: Inertial pitch link load mapping

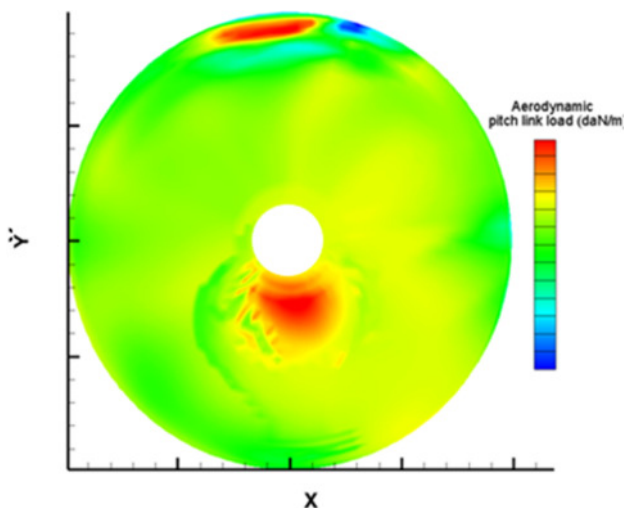


Figure 11: Aerodynamic pitch link load mapping

That is the reason why the load is mostly created near the blade tip.

Concerning the retreating blade area's oscillations, they are created in the current part of the blade and caused by a blade's torsional elastic response. During the advancing blade sector, the blade is subject to high torsional deformation that, once released, can react along the retreating blade sector.

In Figure 11 the aerodynamic part of the pitch link load shows interesting areas in the advancing blade sector and in the reversed flow disc. The advancing blade area is subject to transonic phenomena. Actually the first area near  $\psi=80^\circ$  is created by a  $C_m$  divergence caused by the Mach rising. In this area the AoA does not change so much before the advancing blade's position ( $\psi=90^\circ$ ) after which the cyclic pitch command tends to decrease the AoA that can reach values below zero. This low AoA value but still near zero creates a lift projection in leading edge direction. This is possible because the zero lift AoA is around  $-1^\circ$ . The blade bending deformation creates a lever arm with this projected force that creates the aerodynamic pitch link traction at  $\psi=110^\circ$ . The load mapping allows to clearly see the load repartition along the blade and for every azimuth.

## 6. CONCLUSION AND FUTURE WORK

This paper has shown our new computation method and the use of a new post-processing tool in order to analysis pitch link loads. Areas that create loads are clearly visible. It will help us understanding differences between calculations and flight-tests results. This new tool will be integrated in the HOST code. This way of working was led by our desire to avoid empirical models. This modeling base has been used for a high-speed forward flight in gyrodyne conditions. Nevertheless, this calculation method has not been compared to flight test results because the helicopter has not flown yet. Flight tests will be the opportunity to bring computation results and flight test data face to face, and to close the loop concerning the load prediction state of the art.

## 7. REFERENCES

- [1] B. Benoit, K. Kampa, P.-M. Basset, W. Von Grünhagen, and B. Gimonet, "HOST, a General Helicopter Simulation Tool for Germany and France," 2000.
- [2] P.-M. Basset, "Application of the Finite State Unsteady Wake Model in Helicopter Flight Dynamic Simulation.
- [3] M. Allongue and T. Krysinski, "Modélisation de la Pale souple utilisée dans le programme R85," Aérospatiale - Division Hélicoptères, H/DE.M 209/87, 1987.
- [4] M. Paris, "Identification du comportement en torsion à fort facteur d'avancement des pales d'hélicoptère conventionne : application à la réduction des efforts de commandes sur une formule hybride haute vitesse de type X3," Paris, ENSAM, 2014.
- [5] B. Benoit, G. Arnaud, and F. Toulmay, "Amélioration du modèle aérodynamique du code rotor hélicoptères R85 validation et application," presented at the 28<sup>ème</sup> Colloque d'Aérodynamique appliquée I.S.L, Oct. 1991.
- [6] T. Theodorsen, "General Theory of Aerodynamic Instability and the Mechanism of Flutter," Jan. 1949.
- [7] N. Kruppa, "Unsteady aerodynamics in an Aeroelastic Rotorcraft Simulation Tool," Technical University of Denmark.
- [8] F. J. Tarzanin, "Prediction of Control Loads Due to Blade Stall," Apr. 01, 1972.
- [9] R. T. N. Chen, "A survey of nonuniform inflow models for rotorcraft flight dynamics and control applications," presented at the 15th European Rotorcraft Forum, Amsterdam, Netherlands, Nov. 1989.
- [10] M. Mudry, "La théorie générale des nappes et filaments tourbillonnaires et ses applications à l'aérodynamique instationnaire," Phd Thesis, Université Pierre et Marie Curie (Paris VI), 1982.
- [11] I. Gonzales-Martino, "Development of Moderate-Cost Methodologies for the Aerodynamic Simulation of Contra-Rotating Open Rotors," UPMC, 2014.